eSim 2018
«BUILDING SIMULATION TO SUPPORT BUILDING SUSTAINABILITY»
IBPSA Canada
The Canadian Chapter of the International Building Performance Simulation Association
Le chapitre canadien de International Building Performance Simulation Association

# Scale Modelling of Ventilative Buildings

Dahai Qi[1,2], Xin Zhang[1], Cheng Zhang[1], Andreas Athienitis[1], Liangzhu Wang[1]

[1] Centre for Zero Energy Building Studies, Department of Building, Civil and Environmental Engineering, Concordia University, Montreal, Quebec, Canada
[2] Department of Civil and Building Engineering, Université de Sherbrooke, Sherbrooke, QC, Canada

***Abstract:*** *Free cooling from natural ventilation is an effective energy saving measure. Understanding naturally-driven airflow is important because it is directly related to its efficiency of heat removal. While full-scale building tests reflect a real-world scenario of a ventilative building, they are often costly and time consuming, more importantly, complicated by many uncertainties in the field. In comparison, sub-scaled experiments provide a faster evaluation of the underlying physics at a much less cost. However, the proper scaling is unavailable from the literature. This study aims to develop a series of new scaling methods of thermal airflows in ventilative buildings supported by both experimental studies and numerical simulations of the sub-scale model and the corresponding full-scale building. Comparison of the sub-scale experiments and the full-scale simulations showed that the new scaling methods are able to conserve thermal airflow physics properly at both scales.*

***Keywords:*** *Scale modelling, ventilative buildings, experimental, numerical*

## INTRODUCTION

Buildings consume a huge amount of energy, accounting for around 41% of the primary energy usage for residential, commercial and institutional buildings. More than 55% of the residential sector's energy consumption is for space heating and cooling (OEE, 2011). As an effective approach to remove indoor heat, natural ventilation is often considered as a sustainable and energy saving solution. In Mexico, natural ventilation could achieve an estimated saving of 4.8 TWh/year (Oropeza-Perez and Østergaard, 2014). In an Andalusian school, by simply replacing the mechanical ventilation system with a natural ventilation system, it saves approximate 18-33% of annual energy consumption while maintaining classroom comfort levels (Gil-Baez et al., 2017). Free cooling through natural ventilation is thus widely applied in residential and commercial building sections.

Understanding naturally-driven airflow in buildings is essential because it is directly related to its efficiency of heat removal. It is also essential for the evaluation of natural ventilation during the early stage of building designs, e.g. at the conceptual design stage. Numerical simulation and experiments are the most frequent methods to study and design natural ventilation system in buildings. Ai and Mak investigated single-sided NV in buildings in the urban area. CFD simulations were conducted for room ventilation rate analysis. It shows that the ventilation rate would be decreased up to 67% when the aspect ratio of a street canyon is significantly increased (Ai and Mak, 2018). Cheung and Liu explored the effects of building interference on NV using CFD standard two equation k-ε model (Cheung and Liu, 2011). The cross ventilation rate could be doubled by proper building disposition for NV performance enhancing. Compared to numerical simulations, experiments plays a critical role because, when done properly, experiments provide valuable and realistic data reflecting real-world phenomena and are often used to verify simulation results. Jun et al. conducted full-scale field measurements to study natural and mechanical ventilation in an institutional high-rise building (Cheng et al., 2017). However, full-scale and long-term measurements of ventilation in buildings are costly and even impractical especially for large buildings so sub-scaled experiments thus apply (Chen, 2009). Walker et al. developed a 1:12 reduced-scale building to investigate the buoyancy-driven natural ventilation regarding temperature and natural ventilation flow rate (Walker et al., 2011). Zhou et al. did a scale chamber test (1 m × 1 m × 1 m) studied the particle dispersion in a ventilated and floor-heated indoor environment (Zhou et al., 2017). However, few of the previous studies validated the scaling methods. Saltwater modeling is often used to design small scale natural ventilation experiments (Gladstone and Woods, 2001; Linden, 1999). The idea of saltwater modeling is to substitute turbulent buoyant salt water moving in fresh water for turbulent buoyant warm air moving in cold gas (Steckler et al., 1986). The scale model is submerged in a tank of fresh water and the injected salt water simulates a heat source. Since the density of salt water is higher than fresh water, the salt water tends to flow down whereas warm air to flow upward. However, this scaling approach neglects heat transfer through surrounding walls and could not model heat transfer process properly.


ISBN 978-2-921145-88-6

This study aims to develop a series of new scaling methods of thermal airflows in ventilative buildings that consider heat transfer through boundary walls. Both experimental studies and numerical simulations of the sub-scale model and the corresponding full-scale building were conducted. Comparison of the sub-scale experiments and the full-scale simulations showed that the new scaling method can conserve thermal airflow physics properly at both scales.

## METHODOLOGY

### Scaling method

As is illustrated in Fig. 1, the internal heat source heats the indoor air and creates stack effect by increasing temperature difference between the inside and outside of the building. Driven by the stack effect, outdoor air enters into the building through the bottom opening and exits via the top opening. In this section, the analytical solution of the heat and mass transfer for the buoyancy-driven natural ventilation building is derived first, then based on the analytical solution, a new scaling method is proposed accounting for the heat transfer between the air and the wall surface, which has been often neglected by previous studies.

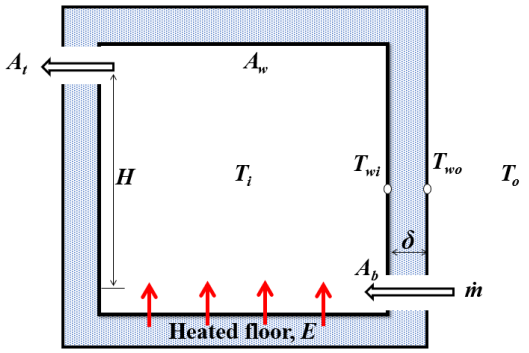


*Figure 1: Schematic of a natural ventilation building*

Airflow movement in buildings is a complex phenomenon, and it is difficult to keep the air distribution the same between small scale and full-scale buildings. The key point of scaling is to keep the most important parameters that our study focuses, e.g. the indoor temperature. Therefore, simplification of the building physics is necessary in the similarity analysis, where the assumption of well mixed medium, e.g. air, gas or water, is often used, like the development of Froude modeling approach and salter water modeling approach (Klote et al., 2012) to keep stack effect similar in buildings. The key parameters here are the indoor air temperature and the flow rate of ventilation, which are obtained by solving the energy equation and mass flow equations in Eqs. (1) and (2), under the following assumptions: the indoor air is well mixed, static and at steady state with surrounding wall surface temperature kept as constant and uniform.

Energy Equation

$$\dot{m}C_p(T_i - T_0) + UA_W(T_i - T_0) = E \quad (1)$$

Where, $U = \dfrac{1}{1/h_{wi} + \delta/k + 1/h_{wo}}$

$\dot{m}$ is the mass flow rate; $T_i$ and $T_o$ are the indoor and outdoor temperature, respectively. $A_t$ and $A_b$ are the top and bottom opening area. The vertical distance between these two openings is $H$. $E$ is the heat source of heated floor. $T_{wi}$ and $T_{wo}$ are the interior and exterior wall surface temperature. $A_w$ is the wall surface area. $h_{wi}$ and $h_{wo}$ are the heat transfer coefficient at the interior and exterior wall surfaces. $\delta$ is the wall thickness; $k$ is the heat conductivity coefficient.

Mass flow rate equation:

$$\dot{m} = C_d A^* \sqrt{2gH\frac{T_i - T_0}{T_0}\rho_0} \quad (2)$$

Submitting (2) into (1), Eq. (3) can be obtained:

$$\frac{\Delta T}{T_0} = \frac{\alpha}{\sqrt{\dfrac{\Delta T}{T_0}} + \beta} \quad (3)$$

Where, $\alpha$ and $\beta$ are dimensionless numbers:

$$\alpha = \frac{E}{C_d\sqrt{2gH}\rho_0 C_p A^* T_0} \quad (4)$$

$$\beta = \frac{UA_W}{C_d\sqrt{2gH}\rho_0 C_p A^*} \quad (5)$$

$\Delta T$ is the indoor and outdoor temperature difference. $C_d$ is the discharge coefficient accounting for the total flow resistances including that at the openings and building interior structure; $A^* = A_t A_b / \sqrt{A_t^2 + A_b^2}$ is the effective areas of $A_t$ and $A_b$. $\rho_o$ is the outdoor air density. $C_p$ is the heat capacity of air. The dimensionless number $\alpha$ is related to the value of heat source and building geometry, $E$, so it represents dimensionless heat source. $\beta$ is determined by the value of thermal resistance of building walls and building geometry, so it represents dimensionless building property.

Solutions to the temperature and mass flow rate could be obtained by solving Eqs. (3), which is only the function of dimensionless numbers $\alpha$ and $\beta$. It indicates that once the dimensionless numbers $\alpha$ and $\beta$ are conserved between different scale building models, the dimensionless temperature and the dimensionless mass flow rate will be


ISBN 978-2-921145-88-6

conserved among different scales as shown by Eqs. (6) and (7).

- Dimensionless air temperature:

$$\left(\frac{\Delta T}{T_0}\right) = f(\alpha, \beta) \tag{6}$$

- Dimensionless mass flow rate:

$$\frac{\dot{m}}{A^* \rho_0 \sqrt{2gH}} = C_d \sqrt{\frac{\Delta T}{T_0}} = f(\alpha, \beta) \tag{7}$$

That is to say: for two buildings at different scales, e.g. the scaled model (m), and the full-size building (f), $\alpha_m = \alpha_f$ and $\beta_m = \beta_f$. As a result, the required opening areas and the heat release rate should satisfy Eqs. (8) and (9).

Opening area to satisfy $\beta_m = \beta_f$:

$$\frac{A^*_m}{A^*_f} = \frac{U_m A_{W,m} C_{d,f} \sqrt{H_f} \rho_{0,f}}{U_f A_{W,f} C_{d,m} \sqrt{H_m} \rho_{0,m}} \tag{8}$$

Where A is the opening area, subscript *m* means scaled model and *f* means full size.

Heat release rate for $\alpha_m = \alpha_f$:

$$\frac{E_m}{E_f} = \frac{C_{d,m} \sqrt{H_m} \rho_{0,m} C_{p,m} A^*_m T_{0,m}}{C_{d,f} \sqrt{H_f} \rho_{0,f} C_{p,f} A^*_f T_{0,f}} \tag{9}$$

Conserve the number of $\alpha$ and $\beta$, the projected mass flow rate of sub-scaled model to full-size model can be obtained:

$$\dot{m}_f = \frac{C_{d,f} A^*_f \rho_{0,f} \sqrt{H_f}}{C_{d,m} A^*_m \rho_{0,m} \sqrt{H_m}} \dot{m}_m \tag{10}$$

## Simulation Setup

To verify the scaling method, different scale building models were designed based on the new scaling method proposed in this study and were simulated by ANSYS FLUENT under steady state conditions. FLUENT has been widely applied in the building thermal flow studies (Goubran et al., 2016; Lian and Qi, 2009; Qi et al., 2015).

Steady-state simulations were conducted on two different scale building models shown in Table 1. The large scale building model is with the same geometry with the case from the literature Li et al. (2001) as is shown in Fig. 2, which is a 1:50 scaled model. The small scale building model is half size of the large one. Table 1 lists the material and thermal property of the wall, as well as the heat source for the simulation cases. The ground floor is set up as the heat source.

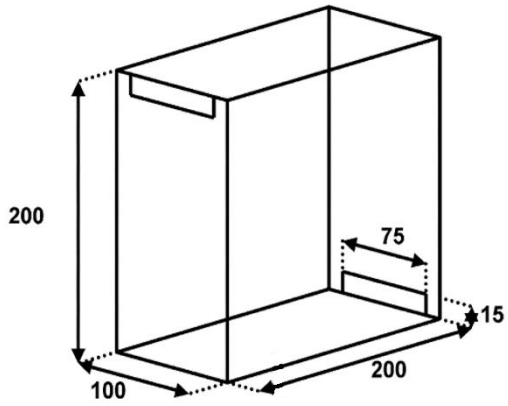


*Figure 2. Illustration of the large size building model (Unit: mm)* (Li et al., 2001).

For the small scale model, the grid size of the inlet and outlet is 0.0015 m×0.0015 m and in other regions coarser grids with the size of 0.002 m×0.002 m are applied. The total number of the grids is about 110,000. In comparison, for the large scale model, the grid size of the inlet and outlet is 0.002 m×0.002 m, and the coarser grids are with the size of 0.004 m×0.004 m so the total number of the grids is about 190,000. The standard k-ε turbulence model is selected as the turbulence model and the pressure-velocity coupling adopts SIMPLE algorithm (Lian et al., 2010; Wang and Zhong, 2014). k-ε turbulence is widely used to simulate buoyancy driven natural ventilation. Walker et al. used k-e turbulence model to simulate buoyancy driven natural ventilation in a small scale building and compared the results with the measurement data (Walker et al., 2011). Yang et al. applied k-e turbulence model to investigate the airflow characteristics and thermal comfort in buoyancy-driven natural ventilation rooms (Yang et al., 2015).

*Table 1. Steady state simulation cases.*

| | **Small size (H=0.1 m)** | **Large size (H=0.2 m)** |
|---|---|---|
| Material | Polylactic acid | Acrylic board |
| Top and bottom opening, m × m | 0.044×0.009 | 0.075×0.015 |


ISBN 978-2-921145-88-6

| | | |
|---|---|---|
| Heat conductivity [W/m·K] | 0.2 | 0.13 |
| Wall thickness, m | 0.008 | 0.008 |
| Heat source power, W | 0.5 ~ 2.75 | 2 ~11 |

## RESULTS

To validate CFD modeling, a cubic chamber is built which is with the same size and geometry with the case from the literature Li et al. (2001) as is shown in Fig. 3. The side walls without inlet and outlet openings are made of acrylic plane with thickness of 11 mm. The other side top walls are made of polylactic acid with thickness of 12.3 mm through 3D printing. The floor is wood and is 33 mm thick. Two light bulbs were installed in the floor as the heater, and was measured 12 W. An iron plate covers on the bulbs to achieve even distributed heat flow from the floor.

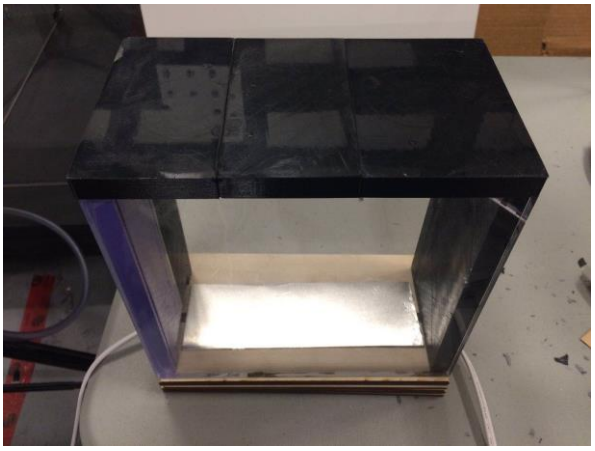

*Figure 3. Experimental chamber.*

According to the flow pattern obtained from CFD simulation (Fig. 4), four thermocouples are distributed inside the chamber to measure temperature as shown in Fig. 4. P1, P2 are located near the main stream and P4 is at the top opening. The thermocouples are type T copper-constantan with the accuracy of ± 0.5 ˚C. Table 3 compares the temperature rise measured by the thermocouples, which shows that the simulation results are close to the experimental data. There exist some discrepancies, e.g. P2. This could be caused by the constant and uniform physical properties of the walls used in the simulations whereas they are actually not the case in the 3D printed walls, where non-uniform properties exist as a result of the 3D printing process. Therefore, the CFD modeling method is partially validated. To do a full validation, Particle image velocimetry (PIV) will be applied to capture the natural of the flow, e.g. velocity profile inside of the chamber. Moreover, the gas analyzers will also be used to measure flow rate of natural ventilation. The results of the tests will be compared with the CFD simulation results in the future. The grid independent study will be further conducted and compared with the results from PIV and Gas Analyzers test in the future.

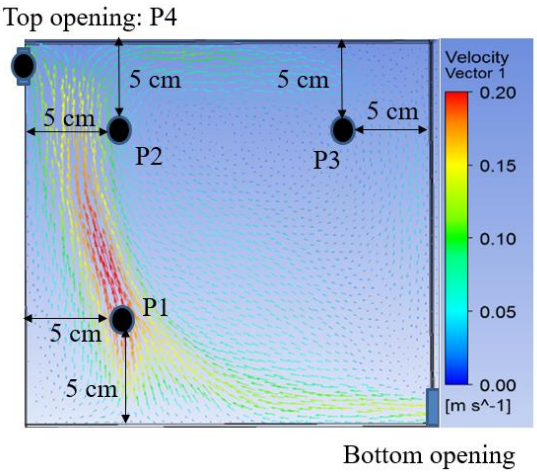


*Figure 4. Flow pattern (CFD) and distribution of thermocouples.*

*Table 3: Comparison of measured and simulated temperature rise (°C).*

| | P1 | P2 | P3 | P4 |
|---|---|---|---|---|
| Exp. | 17.5 | 8 | 7.5 | 5 |
| CFD | 16 | 5.2 | 5 | 6 |

To verify the new scaling method, the simulated outlet temperature and mass flow rate of small scale and large scale building models are compared. Fig.5 compares the simulated outlet temperatures of the small scale and large scale building models to, as well as that of the dimensionless temperature solution to solved by Eq. (3) at different heat sources. The largest difference of outlet air temperature between the small and large scale models is 14% (see Fig. 5). Fig. 6 compares the calculated mass flow rates of the small scale and large scale building models to the solutions to Eq. (7). The largest difference is 10%. The differences are probably caused by the uniform indoor temperature assumption in the development of the scaling method, which is applied to the small scale and large scale models design. Considering the natural ventilation is a complex process of heat and mass transfer, the differences are acceptable. Therefore, the temperature and mass flow rate are conserved using the developed new scaling method for the natural ventilation buildings.


ISBN 978-2-921145-88-6

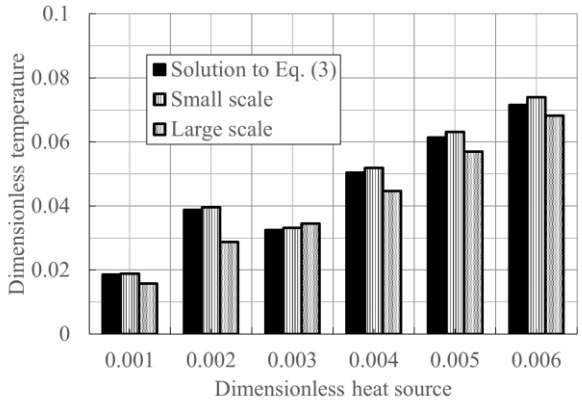


Figure 5. Outlet temperature of small size and large scale building models.

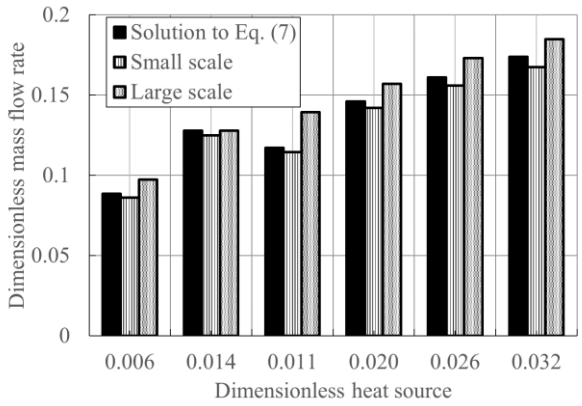


Figure 6. Mass flow rate of small and large scale building models.

It should be noted that the research now is focus on the steady state flow, inculding the analysical model and CFD simulation. Future work will be conducted on deriving transient analytical model. Based on it experimental and CFD study will be designed and the results will be compared.

## CONCLUSION

In order to develop an improved scaling method of ventilative buildings in terms of mass flow rate and temperature, this study derived analytical solutions to the heat and mass transfer in a single-zone building, based on which the new scaling method was proposed. Two different scale building models were designed according to the scaling method and were simulated by CFD. To validate the CFD modelling method, experiments were also conducted. Following conclusions were obtained from this study:

1) The analytical solution shows that the dimensionless indoor temperature and flow rate are decided by two dimensionless numbers, dimensionless heat source, $\alpha$, and dimensionless building property, $\beta$. Therefore, once the two dimensionless numbers can be conserved in different scale building models, dimensionless indoor temperature and flow rate could be maintained.
2) The CFD simulation results indicate that the scaling method proposed based on the analytical solutions can be used to model sub-scale natural ventilation buildings under steady state condition.
3) The results show that the new scaling method can conserve thermal airflow physics properly at both scales.

Further studies will focus on the time scaling method of transient ventilate buildings. Particle image velocimetry (PIV) will be applied to study flow patterns of different scale building models which are designed by the new scaling methods. Moreover, the actual physical meanings of the dimensionless numbers will be further explored.

## REFERENCES

Ai, Z.T., Mak, C.M., 2018. Wind-induced single-sided natural ventilation in buildings near a long street canyon: CFD evaluation of street configuration and envelope design. J. Wind Eng. Ind. Aerodyn. 172, 96–106.

Chen, Q., 2009. Ventilation performance prediction for buildings: A method overview and recent applications. Build. Environ. 44, 848–858.

Cheng, J., Qi, D., Wang, L., Athienitis, A., 2017. Whole-Building Simulation of Hybrid Ventilation based on Full-scale Measurements in an Institutional High-rise Building for Predictive Control, in: Building Simulation 2017. Proceedings of the 15th IBPSA Conference, San Francisco, CA, pp. 1391–1396.

Cheung, J.O.P., Liu, C.H., 2011. CFD simulations of natural ventilation behaviour in high-rise buildings in regular and staggered arrangements at various spacings. Energy Build. 43, 1149–1158. https://doi.org/10.1016/j.enbuild.2010.11.024

Gil-Baez, M., Barrios-Padura, Á., Molina-Huelva, M., Chacartegui, R., 2017. Natural ventilation systems in 21st-century for near zero energy school buildings. Energy 1–15. https://doi.org/10.1016/j.energy.2017.05.188

Gladstone, C., Woods, A.W., 2001. On buoyancy-driven natural ventilation of a room with a heated floor. J. Fluid Mech. 441, 293–314. https://doi.org/10.1017/S0022112001004876

Goubran, S., Qi, D., Saleh, W.F., Wang, L.L., Zmeureanu, R., 2016. Experimental study on the flow characteristics of air curtains at building entrances.


ISBN 978-2-921145-88-6

Build. Environ. 105, 225–235.

Klote, J.H., Milke, J.A., Turnbull, P.G., Kashef, A., Ferreira, M.J., 2012. Handbook of Smoke Control Engineering. American Society of Heating Refrigerating and Air-Conditioning Engineers, Atlanta, GA.

Li, Y., Delsante, A., Chen, Z., Sandberg, M., Andersen, A., 2001. Some examples of solution multiplicity in natural ventilation. Build. Environ. 36, 851–858.

Lian, Z., Qi, D., 2009. Modification for evaluation indexes of air distribution. J. Chongqing Univ. 8, 937–942.

Lian, Z., Qi, D., Weiwei, L., 2010. Influence of indoor partition on air distribution of ceiling-mounted cassette type indoor unit. J. Cent. South Univ. 41, 363–369.

Linden, P.F., 1999. The fluid mechanics of natural ventilation. Annu. Rev. Fluid Mech. 31, 201–238.

OEE, 2011. Secondary Energy Use by End-Use. Off. Energy Effic. Nat. Resour. Canada.

Oropeza-Perez, I., Østergaard, P.A., 2014. The influence of an estimated energy saving due to natural ventilation on the Mexican energy system. Energy 64, 1080–1091. https://doi.org/10.1016/j.energy.2013.11.009

Qi, D., Goubran, S., Zmeureanu, R., Wang, L., 2015. Effect of People on Infiltration of Building Entrance with Air Curtains_updated, in: ISHVAC-COBEE 2015 Conference. ISHVAC-COBEE 2015, Tianjin, p. 9.

Steckler, K.D., Baum, H.R., Quintiere, A.X.J.G., 1986. Multicompartment Enclosures Elements of Salt Water Modeling. Twenty-first Symp. (International)on Combust. Combust. Inst. 143–149.

Walker, C., Tan, G., Glicksman, L., 2011. Reduced-scale building model and numerical investigations to buoyancy-driven natural ventilation. Energy Build. 43, 2404–2413. https://doi.org/10.1016/j.enbuild.2011.05.022

Wang, L.L., Zhong, Z., 2014. An approach to determine infiltration characteristics of building entrance equipped with air curtains. Energy Build. 75, 312–320.

Yang, X., Zhong, K., Kang, Y., Tao, T., 2015. Numerical investigation on the airflow characteristics and thermal comfort in buoyancy-driven natural ventilation rooms. Energy Build. 109, 255–266. https://doi.org/10.1016/j.enbuild.2015.09.071

Zhou, Y., Deng, Y., Wu, P., Cao, S.J., 2017. The effects of ventilation and floor heating systems on the dispersion and deposition of fine particles in an enclosed environment. Build. Environ. 125, 192–205. https://doi.org/10.1016/j.buildenv.2017.08.049


ISBN 978-2-921145-88-6